On the Role of Microcrack Initiation during Fatigue of a Duplex Steel in the Very-High-Cycle-Fatigue (VHCF) Regime

Ulrich Krupp[1*], Helge Knobbe[2], Hans-Jürgen Christ[2], Philipp Köster[3], and Claus-Peter Fritzen[3]

[1]Faculty of Engineering and Computer Sciences, University of Applied Sciences Osnabrück, 49009 Osnabrück, Germany

[2]Institut für Werkstofftechnik, Universität Siegen, 57068 Siegen, Germany

[3]Institut für Mechanik und Regelungstechnik, Universität Siegen57068 Siegen, Germany

[*]u.krupp@fh-osnabrueck.de

Keywords: VHCF, short cracks, fatigue crack initiation, EBSD, modeling.

Abstract. Austenitic-ferritic duplex steels are used for structural applications when high strength in combination with excellent corrosion resistance is required. Many of these applications imply cyclic loading and hence, fatigue damage needs to be considered for dimensioning. Most dimensioning strategies make use of the fatigue-limit concept. However, while the original fatigue-limit concept is based on the idea that existing slip bands or microcracks are blocked by microstructural boundaries like grain or phase boundaries, more recent research work has shown that metallic structures may fail far below the conventional fatigue limit even at very high numbers of cycles to fracture. The present paper deals with the observation of local plasticity and fatigue damage in the VHCF regime by means of high-frequency fatigue testing in combination with scanning electron microscopy (SEM) and with electron back-scattered diffraction (EBSD). The results reveal that fatigue damage in the VHCF regime indeed causes the formation of slip bands followed by initiation and propagation of microstructurally short cracks in a very localized manner, being manifested itself by heat generation. The SEM observations and measurements of slip band geometries were correlated with calculations using a finite-element and a numerical short-crack model, which take the real two-phase microstructure and its elastic/plastic anisotropy into account and allow the prediction of both (i) the fatigue crack initiation sites and (ii) microcrack-propagation rates.

Introduction

Most structural-integrity concepts for dynamically high-loaded components imply the fatigue-limit concept, which is based on the assumption that below a certain stress value no cycle-dependent damage occurs. In the case of bcc carbon steels it is widely accepted that the fatigue limit corresponds with a number of cycles between 10^6 and 10^7 cycles. In the case of fcc materials, e.g. aluminium or copper alloys, a fatigue limit can not be found, since their lower packing density causes a substantially lower critical shear stress to activate dislocation motion and hence, fatigue damage. However, in most practical cases the conventional fatigue limit concept is applied for nearly all engineering metallic materials that experience more than 10^6 cycles during service.
More recently, it has been found that fatigue failure may occur at stresses well below the conventional fatigue limit at numbers of cycles beyond 10^7. The corresponding fatigue regime, which exhibits an increasing technical relevance, has been termed ultra-high-cycle fatigue (UHCF) or very-high-cycle fatigue (VHCF), respectively. Several mechanisms have been suggested to govern fatigue failure during VHCF (cf. [1]): Murakami et al. [2] correlate the fatigue limit with the size and hardness of non-metallic inclusions. At very high numbers of cycles and correspondingly low stress amplitudes the significance of the plane-stress condition at the surface vanishes and

cracks initiate in the interior of the material at inclusions under inert vacuum conditions. Frequently, an optically dark area (ODA) can be found in the fracture surface, forming together with the inclusion a so-called fish-eye, which is often correlated with hydrogen embrittlement during fatigue crack propagation [3]. Within the ODA a microscopically rough granular area appears around the inclusion (fine-granular area (FGA) or granular bright facet (GBF)) which can be attributed to the initiation and coalescence of many microcracks [4]. In the absence of inclusions of a critical size, fatigue damage occurs by the formation of persistant slip bands (PSBs) as suggested by Mughrabi [5] (type I materials contrary to type II materials with crack initiation at internal inclusions). The conventional fatigue limit corresponds to the PSB limit. However, even below the PSB limit slip irreversibility occurs causing the nucleation of slip bands at phase or grain boundaries. This effect is due to the anisotropy of elastic deformation. According to Tanaka and Mura [6], slip irreversibility eventually causes initiation and propagation of microstructurally short fatigue cracks (cf. [7]). If the applied stress amplitude is not sufficient to make one of these cracks overcoming the adjacent grain or phase boundary, the conventional fatigue limit is reached. As long as irreversible dislocation motion is not completely eliminated, very localized accumulation of plastic slip remains possible and fatigue failures at very high numbers of cycles (N_f<10^7) can be observed. Thus, there should be an absolute fatigue limit, i.e., the irreversibility limit. This is schematically shown in Fig. 1.

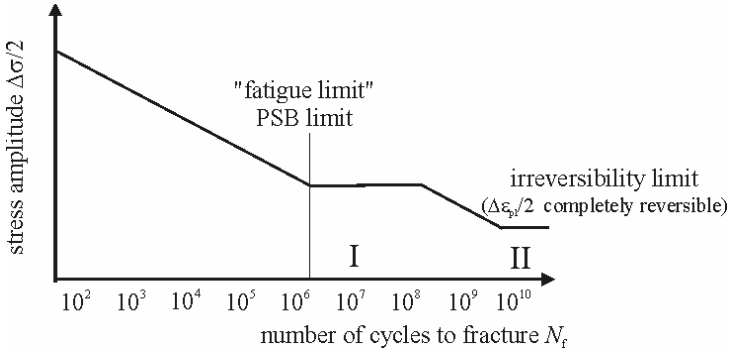

Fig. 1: Two-stage S/N diagram covering both the conventional fatigue limit and the irreversibility limit.

While one can clearly distinguish between the VHCF behaviour of bcc materials and fcc materials, the situation is more complex and not fully understood in the case of two-phase materials showing both lattice structures. In the present study, the VHCF behaviour of an austenitic-ferritic duplex steel is discussed with the focus on the mechanisms of fatigue crack initiation. Predominantly, cracks nucleate at slip bands at austenite/ferrite phase boundaries at the surface, only a few specimens showed sub-surface crack initiation at non-metallic inclusions. These observations are only partially in agreement with the work of Chai [8] on several duplex steels. He observed crack initiation exclusively underneath the surface mostly at non-metallic inclusions.

Experimental Details

The behaviour of microstructurally short fatigue cracks was studied by means of an austenitic (γ) - ferritic (α) duplex steel X2 CrNiMoN 22 5 3 (1.4462). The chemical composition of the material is given in Table 1.

Table 1: Chemical composition of the duplex steel used in this study (wt.%)

Fe	C	Cr	Ni	Mo	Mn	N	P	S
bal.	0.02	21.9	5.6	3.1	1.8	0.19	0.023	0.002

After a 4h-homogenization heat treatment at 1250°C followed by slow-cooling to 1050°C and quenching in water, the microstructure consists of approximately 50% austenite with a mean grain size of 46µm and a Vickers hardness of 263HV embedded in 50% ferrite with a mean grain size of 33µm and a Vickers hardness of 280HV. Fig. 2 shows the microstructure of the duplex steel after heat treatment.

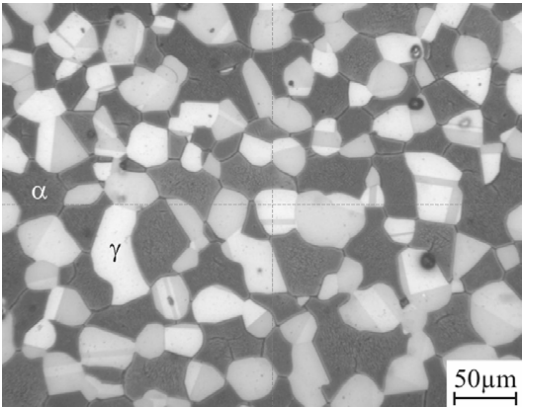

Fig. 2: γ-austenite and α-ferrite microstructure of the duplex steel used in this study.

Push-pull fatigue tests (stress control, stress ratio: R=-1 (R=0)) were carried out on a high-frequency servohydraulic testing system (MTS 810, 1000Hz) and a resonance testing system (Rumul Testtronic) using cylindrical specimens with a diameter of 5mm and 7mm, respectively. Prior testing, the specimens were ground and electro-polished to eliminate any roughness effects on fatigue and to allow the application of the automated EBSD technique (electron back-scattered diffraction) during surface characterization by scanning electron microscopy (SEM). In addition to SEM, slip activity in the different phases were studied by means of transmission electron microscopy (TEM).

Results and Discussion

The results of the fatigue tests are summarized in the S/N diagram in Fig. 3. At a stress level between $\Delta\sigma/2$=380MPa and $\Delta\sigma/2$=385MPa three different situations were observed: (i) crack initiation at slip bands at the surface, (ii) crack initiation at a non-metallic inclusion (fish eye), and (iii) no crack initiation (run-out specimens). Specimens were considered as run-out specimens when a number of cycles of N=10^8 or $5\cdot10^7$ was exceeded. This limitation was necessary because of an excessive heat generation when loading the specimens at frequencies above f=300Hz. It is worth mentioning that even at stress amplitudes (σ=350MPa, run-out N>10^8 cycles) clearly below the macroscopic yield strength of $R_{p0.2}$=420MPa a substantial temperature increase was measured. This observation hints to the fact that plastic slip is not only active throughout the experiment but also by a considerable amount reversible. In a recent paper Wagner et al. [9] correlated the evolution of the

specimen temperature with plasticity-induced energy-dissipation and crack initiation (strong temperature increase) during VHCF. A clear correlation between an increase in the specimen temperature and the occurrence of irreversible fatigue damage could not be derived.

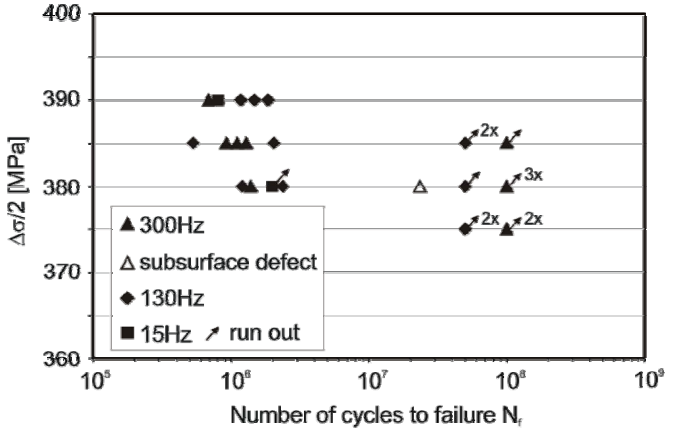

Fig. 3: S/N (Wöhler) diagram of the duplex steel 1.4462.

Figure 4 shows characteristic fracture surfaces of specimens where failure sets in by microstructurally short fatigue cracks. The crystallographic surface crack path in Fig. 4a (showing both: crack path and corresp. fracture surface) shows a different propagation behaviour in the austenite and the ferrite phase, respectively. While crack advance in the ferrite grains is restricted to individual slip bands ② the lower critical shear stress in the austenite grains promote crack advance by operating multiple slip systems ① (cf. [7]). Fig. 4b gives an example of internal crack initiation at a non-metallic inclusion (Al_2O_3). The grained structure around the inclusion reflects the original alloy microstructure, i.e., fatigue damage after crack initiation at the inclusion is governed by the propagation behaviour of microstructurally short fatigue cracks. The corresponding crystallography-oriented roughness is the origin of the fish-eye appearance of the internal crack-initiation site.

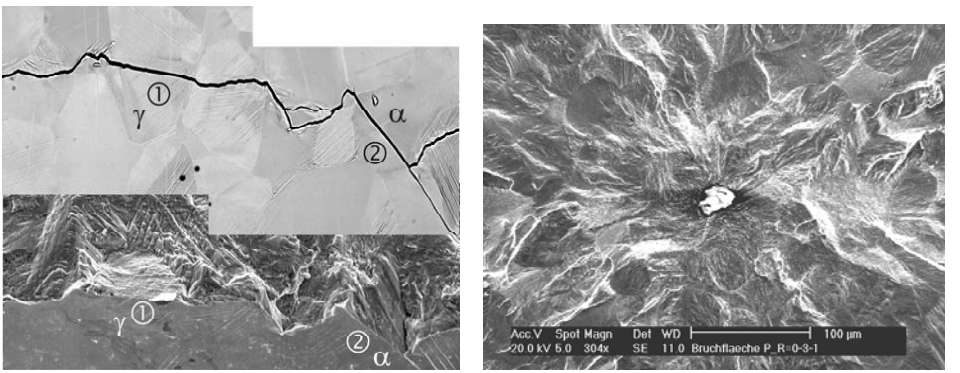

Fig. 4: Fracture surface of fatigue specimens of duplex steel: (a) failed after $N_f \cong 10^6$ cycles at $\Delta\sigma/2$=430MPa and (b) failed after $N_f \cong 10^8$ cycles at $\Delta\sigma/2$=285MPa (R=0).

SEM examination of the run-out specimens (cf. Fig. 3) revealed in all cases some localized traces of plastic deformation. This is shown in Figs. 5 to 7. The quantification of the distribution of the crystallographic orientations in the austenite and ferrite grains of the duplex steel by automated EBSD allowed the determination of the spatial distribution of the relevant slip systems and the calculation of the respective shear stresses (this is described in detail in [10]). The latter required the application of the FE method in combination with a material model that takes elastic anisotropy and crystal plasticity into account. The results are qualitatively in good agreement with the experimental observations. Fig. 5c shows stress maxima in the austenite grain (1) indeed exhibiting slip bands (Fig. 5a).

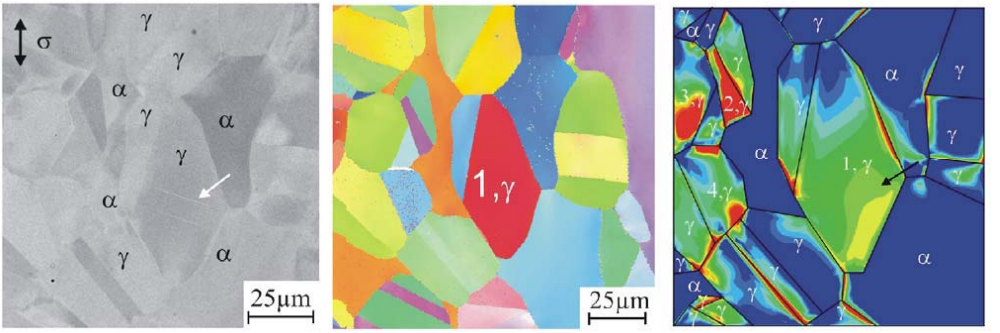

a b c

Fig. 5: (a) Slip bands (arrow) on the surface of a non-failed fatigue specimen of duplex steel, (b) corresponding EBSD map and (c) FE calculation of the maximum resolved shear stresses on the shear planes of the grains evaluated by SEM in (a) and (b).

Figure 6 and 7 shows the local appearance of slip bands during VHCF of duplex steel. The different behaviour of austenite and ferrite grains becomes obvious: In the early stage of fatigue damage, plastic deformation is strictly limited to the softer austenite phase (see arrow in Fig. 6a). Additionally, the phase boundaries act as strong barriers towards the transmission of dislocation motion, as revealed by Fig. 6b.

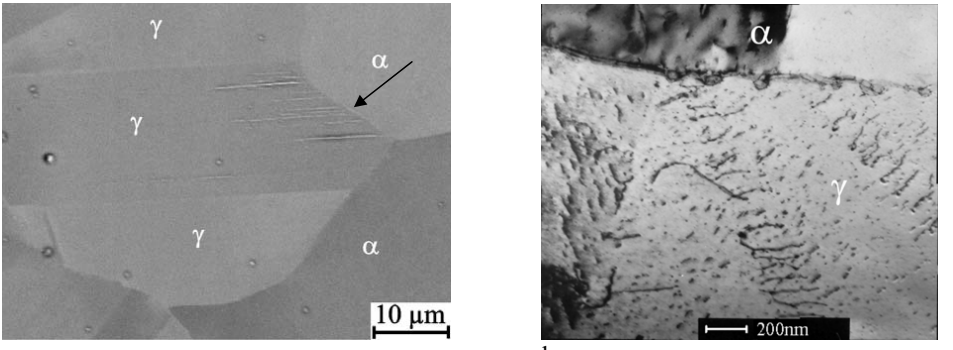

a b

Fig. 6: Plastic deformation limited to the austenite phase: (a) SEM micrograph of slip bands emanating from a ferrite/austenite phase boundary into an austenite grain (b) TEM micrograph of planar arranged dislocations at a ferrite/austenite phase boundary.

While grain boundaries and, in particular, phase boundaries, act as efficient barriers towards slip transmission, twin boundaries seem to exhibit no blocking effect, as it is clearly demonstrated in Fig. 7. Taking into account that the barrier strength of grain boundaries should increase with an increasing misorientation angle between neighbouring grains this result is surprising. A possible explanation could be based on the fact that a twin boundary is a 60° pure tilt boundary. The main contribution of the dislocation blocking effect however is due to the twist misorientation causing an intrinsic resistance to slip transmission.

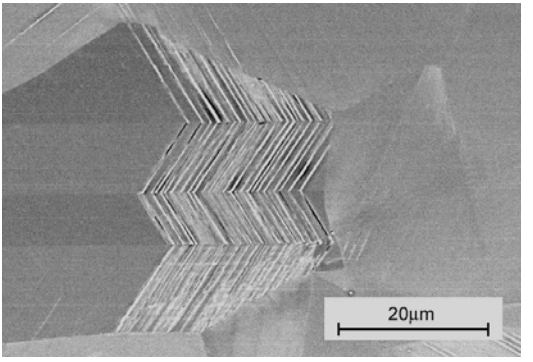

Fig. 7: Slip band formation across twin boundaries in run-out specimens after 10^8 cycles.

The observation of slip bands and slip band cracking has been included in a two-dimensional numerical short crack model, which is explained in more detail in [7,11]. The model considers fatigue crack propagation as being driven by single slip which is represented by a yield-strip approach where the crack and the adjacent crystallographic slip bands are being meshed by boundary elements. When applying an external load, the displacement field along the yield strip and the crack can be calculated. Assuming the shear displacement at the crack tip ($\Delta CTSD$, crack-tip slide displacement) being the governing driving force for crack advance, the crack-propagation rate da/dN can be calculated as

$$\frac{da}{dN} = C\Delta CTSD \,. \tag{1}$$

with the constant C representing the degree of slip irreversibility of $\Delta CTSD$ during one complete loading cycle (in this study: C=0.005). The advantages of a numerical model as compared to the analytical ones, e.g. by Navarro and de los Rios [12] or Tanaka et al. [6] are: (i) the real microstructure including crystallographic orientations and stereographic parameters of the two-phase arrangement is represented by two-dimensional Voronoi cells, (ii) crack path and local crack propagation rates are not input parameters but are calculated according to the local crystallographic orientation relationship, (iii) depending on the critical shear stress of the respective phase (which can be experimentally derived by a Hall-Petch analysis) crack propagation can be driven by single slip (CTSD) or double slip (CTOD) with different contributions of crack closure (cf. [7,10,13]).
Figure 8 gives an example of the application of the model to microstructural fatigue cracks growing in stage 1a (single slip) and stage 1b (double slip). Once the plastic zone ahead of the crack tip becomes larger than one grain diameter, stage II propagation is assumed to prevail, i.e. long fatigue cracks, where the Paris law of linear elastic fracture mechanics is applicable. From Fig. 8 it

becomes obvious that the model reproduces the experimentally observed oscillations in the crack propagation rate, which vanishes during the stage I to stage II transition.

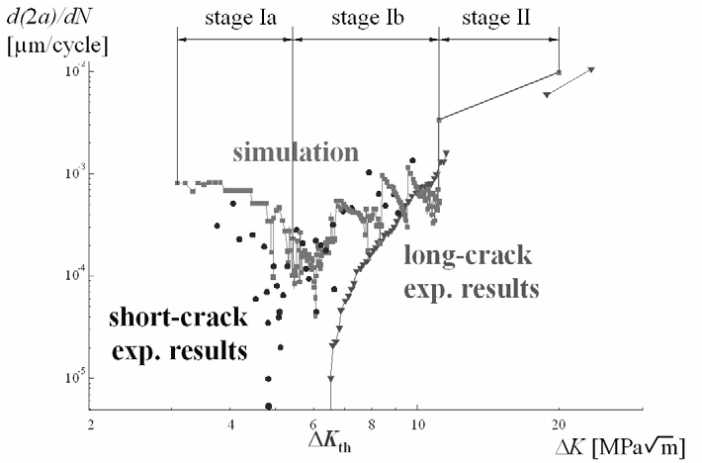

Fig. 8: Experimentally measured and simulated crack propagation rates *da/dN* vs. stress intensity factor ΔK (cf. [7,11]).

When applying the model to synthetic microstructures representing the real scatter in grain, phase and orientation distribution and assuming instable crack propagation (ductile rupture) to occur once the crack length exceeds a critical value, S/N data can be predicted. Figure 9 shows a comparison between the experimental and the calculated numbers of cycles to fracture. The good agreement supports the hypothesis that the strong scatter, which is characteristic for fatigue lives in the HCF and the VHCF regime, can be attributed to the spatial distribution of microstructural barriers of various strengths.

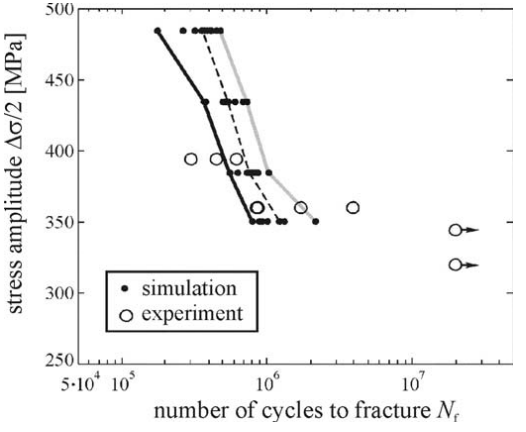

Fig. 9: S/N (Wöhler) diagram for the HCF regime showing a comparison between experimental and simulated results [7,11] (only results of the tests at stress amplitudes between 350MPa and 400MPa can be compared; slightly different specimen geometry than in Fig. 3).

Conclusions

Fatigue damage in the high-cycle and the very high-cycle fatigue regime (HCF and VHCF, resp.) of an austenitic-ferritic duplex steel is governed by the microstructural distribution of the alloy phase patches, grains and crystallographic orientation relationships. In general, first occurrence of plastic slip can be observed in the softer fcc austenite phase. Whether plasticity proceeds to neighbouring grains of the same or a different phase depends on the twist misorientation. Pure tilt grain boundaries, e.g. twin boundaries, seem to have a negligible resistance to slip transmission. Slip activity was found to occur even at low stress amplitudes corresponding to numbers of cycles of $N>10^8$ without fracture. It is postulated that once slip bands are formed, cyclic slip irreversibility causes fatigue failure sooner or later (even at numbers of cycles in the range of 10^9 and more). This kind of damage development, which is strongly determined by the microstructural arrangement within the alloy, can be qualitatively described by a short crack model that has been developed based on the boundary element method. The results are in good agreement with the experimental observation and provide a new tool to support the development of fatigue-resistant tailored microstructures.

References

[1] H. Tian, M.J. Kirkham, L. Jiang, B. Yang, G. Wang and P.K. Liaw, in: Proc. 4th Intl. Conf. on Very High Cycle Fatigue (2007) Ann Arbor, USA, p. 437.
[2] Y. Murakami and M. Endo, Intl. J. Fatigue Vol. 16 (1994) p. 163.
[3] Y. Murakami, T. Nomoto, and T. Ueda, fatigue Fract. Engng Mater. Struct. Vol. 23 (2000) p. 893 & p. 903.
[4] K. Shiozawa, S. Nishino, K. Yamamoto and L. Lu, in: Proc. 8th Intl. Fatigue Congress (2002) Stockholm, Sweden, EMAS Publ., p. 2939.
[5] H. Mughrabi, in: Proc. Intl. Conf. on Fatigue (2006) Atlanta, USA, on CD ROM.
[6] K. Tanaka and T. Mura, T.: J. Appl. Mech. Vol. 48 (1981) p. 97.
[7] U. Krupp: *Fatigue Crack Propagation in Metals and Alloys* (Wiley VCH, Weinheim 2007).
[8] G. Chai: Intl. J. Fatigue Vol. 28 (2006) p. 1533.
[9] D, Wagner, N. Ranc and C. Bathias, in: Proc. 4th Intl. Conf. on Very High Cycle Fatigue (2007) Ann Arbor, USA, p. 101.
[10] O. Düber, B. Künkler, U. Krupp, H.-J. Christ and C.-P. Fritzen: Intl. J. Fatigue, Vol. 28 (2006) p. 983.
[11] B. Künkler: *Mechanismenorientierte Lebensdauervorhersage unter Berücksichtigung der Mikrostruktur*, Fortschritt-Berichte VDI, Nr. 312, (VDI-Verlag, Düsseldorf 2007).
[12] A. Navarro and E.R de Los Rios: Phil. Mag. Vol. 57 (1988) p. 15.
[13] O. Düber: *Untersuchungen zum Ausbreitungsverhalten mikrostrukturell kurzer Ermüdungsrisse in zweiphasigen metallischen Werkstoffen am Beispiel eines austenitisch-ferritischen Duplexstahls*, Fortschritt-Berichte VDI, Nr. 730, (VDI-Verlag, Düsseldorf 2007).